

PROCEEDINGS OF SPIE

SPIEDigitalLibrary.org/conference-proceedings-of-spie

Thoracic lymph node station recognition on CT images based on automatic anatomy recognition with an optimal parent strategy

Guoping Xu, Jayaram K. Udupa, Yubing Tong, Hanqiang Cao, Dewey Odhner, et al.

Guoping Xu, Jayaram K. Udupa, Yubing Tong, Hanqiang Cao, Dewey Odhner, Drew A. Torigian, Xingyu Wu, "Thoracic lymph node station recognition on CT images based on automatic anatomy recognition with an optimal parent strategy," Proc. SPIE 10574, Medical Imaging 2018: Image Processing, 105742F (2 March 2018); doi: 10.1117/12.2293258

SPIE.

Event: SPIE Medical Imaging, 2018, Houston, Texas, United States

Thoracic lymph node station recognition on CT images based on automatic anatomy recognition with an optimal parent strategy

Guoping Xu^{a,b}, Jayaram K. Udupa^{a,*}, Yubing Tong^a, Hanqiang Cao^b
Dewey Odhner^a, Drew A. Torigian^a, Xingyu Wu^a

^aMedical Image Processing Group, 602 Goddard building, 3710 Hamilton Walk, Department of Radiology, University of Pennsylvania, Philadelphia, PA 19104 United States

^bSchool of Electronic Information and Communications, Huazhong University of Science and Technology, Wuhan, Hubei 430074, China

*Corresponding author email: jay@mail.med.upenn.edu

ABSTRACT

Currently, there are many papers that have been published on the detection and segmentation of lymph nodes from medical images. However, it is still a challenging problem owing to low contrast with surrounding soft tissues and the variations of lymph node size and shape on computed tomography (CT) images. This is particularly very difficult on low-dose CT of PET/CT acquisitions. In this study, we utilize our previous automatic anatomy recognition (AAR) framework to recognize the thoracic-lymph node stations defined by the International Association for the Study of Lung Cancer (IASLC) lymph node map. The lymph node stations themselves are viewed as anatomic objects and are localized by using a one-shot method in the AAR framework. Two strategies have been taken in this paper for integration into AAR framework. The first is to combine some lymph node stations into composite lymph node stations according to their geometrical nearness. The other is to find the optimal parent (organ or union of organs) as an anchor for each lymph node station based on the recognition error and thereby find an overall optimal hierarchy to arrange anchor organs and lymph node stations. Based on 28 contrast-enhanced thoracic CT image data sets for model building, 12 independent data sets for testing, our results show that thoracic lymph node stations can be localized within 2-3 voxels compared to the ground truth.

Keywords: Thoracic lymph node zones, fuzzy model, nodal zone localization, automatic anatomy recognition.

1. INTRODUCTION

Accurate assessment of lymph nodes plays an important role in the clinical diagnosis, staging, and response assessment of patients with cancer [1]. However, lymph node segmentation is challenging, and labor-intensive and prone to variability and error when performed manually on computed tomography (CT) images. Considering the difficulties for detecting, localizing, and segmenting lymph nodes, the International Association for the Study of Lung Cancer (IASLC) defined a thoracic lymph node map with anatomic definitions for all lymph node stations [2] or zones to help standardize thoracic lymph node location and reporting. Automatic localization of nodal zones has many potential applications in disease staging, response assessment, etc. without explicitly performing node detection and delineation. Based on IASLC-defined lymph node stations, we showed in our earlier work that mediastinal and hilar lymph node stations can be automatically localized on CT images by using a hierarchical fuzzy model and object recognition algorithms [3], although the recognition result was not ideal given that the hierarchy was not optimized for every lymph node station. In [4], the Automatic Anatomy Recognition (AAR) framework [5] was used to recognize the thoracic lymph node stations on positron emission tomography /computed tomography (PET/CT) images. However, that study did not make full use of the information regarding other organs in the thorax to improve the recognition of the lymph node stations.

In comparison to our previous work on lymph node station recognition, two new strategies have been taken in this paper. The first one is to combine some lymph node stations according to their geometrical distance. The other strategy is to

find the optimal parent (organ or union of organs) as an anchor object in our AAR framework for each lymph node station. Subsequently, each lymph node station can automatically be recognized by using AAR framework. Our ultimate goal (not considered in this paper) is to automatically quantify lymph node disease via PET/CT/MRI within each station following recognition without explicitly delineating lymph nodes. Our early results indicate that accurate recognition of nodal zones within 1-2 voxels can facilitate this goal. This is our rationale for accurate recognition of objects and nodal stations.

2. METHODS

Our proposed method to automatically recognize lymph node stations is based on the AAR framework which is designed for body-wide organ modeling, recognition, and delineation [5]. Here, we treat lymph node stations as anatomic objects, but key anatomic organs as anchor objects of reference for nodal zones. In the AAR framework, it is essential to build a hierarchy for arranging all objects (lymph node stations or anatomic organs). Nodal zones behave differently in terms of how they can be characterized in the image, their intensity properties, relationship to other zones and organs, etc. To find a hierarchy that gives the best recognition accuracy for zones, we take the following approach.

For each nodal zone, we determine a mini hierarchy as depicted in Figure 1. The first level of the hierarchy is the root (see Figure 1) which in our case is always the Skin object. The second level (Parent) is an anchor organ, and the nodal zone under consideration constitutes the third level or Child. We allow the Parent to be an organ or unions of different organs. For each given Child (nodal zone), we determine from the training data set the Parent that affords the least recognition error. Subsequently, the determined optimal Parent organs are all strung individually from the Root to form a single hierarchy that is used in the AAR framework.

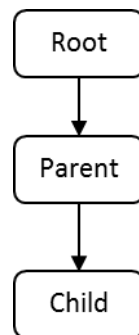


Figure 1: The basic structure of the hierarchy, in which the root is the skin, the parent is composed of an organ or combined organs and the child represents each lymph node station or combined lymph node station.

The methodology is composed of four main steps. Firstly, we find the optimal threshold of each thoracic organ based on a grid search method [5] for facilitating organ localization. Second, following the mini hierarchy, each nodal zone is recognized and based on recognition error, the optimal parent is found. Third, we form a hierarchy as described above involving all organs and zones and then build the fuzzy anatomy model as per this best hierarchy. Finally, we employ this model and the AAR framework to recognize the thoracic nodal zones.

2.1 Finding optimal threshold for each thoracic organ

It is critical to find the optimum threshold of anchor organs for AAR during recognition. In [6], it builds a super mask with the union of all training binary images of the object and makes use of the statistical information of histograms of the

gray image over super mask to estimate the optimum threshold. However, the range of threshold may sometimes shrink into a singular value for some organs like stomach.

Here, we employ a grid search method to change the range of each organ's threshold. Then, the recognition will be done after setting the range of threshold. The method can be described as follows:

- 1) Select an initial range of threshold by using the method in [6]. Determine the start value of the threshold S , the end value of the threshold E , the tolerance range of the threshold of the object from $T1$ to $T2$, and the value of step in each iteration;
- 2) Recognize the organs according to the hierarchy in which the organs are all under the root;
- 3) Change the value of step, and get the new range of threshold for the organ;
- 4) Repeat step 2 and step 3 until the value S is greater than $T1$, and the value E is greater than $T2$;
- 5) Find the best range of threshold in which the recognition error is the least.

2.2 Finding the optimal parent for each lymph node station

The hierarchy for organizing thoracic organs and nodal zones plays an important part in AAR framework. Different results will be obtained by using various hierarchies. Here, we design a method based on the recognition error at training.

The root is the skin outer boundary of the thoracic body region which is usually not hard to localize and delineate [5]. The parent is one of the anatomic organs or combined organs. We have considered 12 basic anatomic organs in the thorax: outer skin boundary of the thoracic body region (tskin), thoracic skeleton (tsk), left and right pleural spaces (lps & rps), trachea and bronchi (tb), pericardium (pc), respiratory system (rs = lps + rps + tb), arterial system (as), esophagus (e), venous system (vs), spinal cord (scord), and internal mediastinum (ims). We combine every two basic anatomic organs (except tskin and tsk) in order to form a set of candidate parents. So, we have 12 basic anatomic organs and 45 combined organs which we employ as parent for each zone.

The child is one of the nodal zones, including: station1, station2L, station2R, station3a, station3p, station4L, station4R, station5, station6, station7, station8, station9, station10L, and station10R according to the IASLC thoracic lymph node map. Here, we combine some stations considering their positional relationships in order to improve the recognition performance and also since some of the zones are very small. As such, we have 8 resulting nodal zones: station12 (station1 + station2L + Station2R), station3 (Station3a + Station3p), station4 (Station4L + Station4R), station56 (station5 + station6), station7, station89 (station8 + station 9), station10R, and station10L.

In order to find the optimal parent for each nodal zone, we take the following strategy: First, we employ the AAR to recognize the objects (organs and combined organs) under the root (tskin) using the mini hierarchy in Figure 1. Next, we recognize each nodal zone under every object. Lastly, we obtain a recognition error matrix which records the recognition error for each nodal zone under every object. Then find the best parent for every nodal zone according to the recognition matrix, in which we can find the least recognition error of the pair-wise parent and child. The final integrated optimum hierarchy for the thorax based on the recognition result of nodal zones that we derived in this manner is shown in Figure 2:

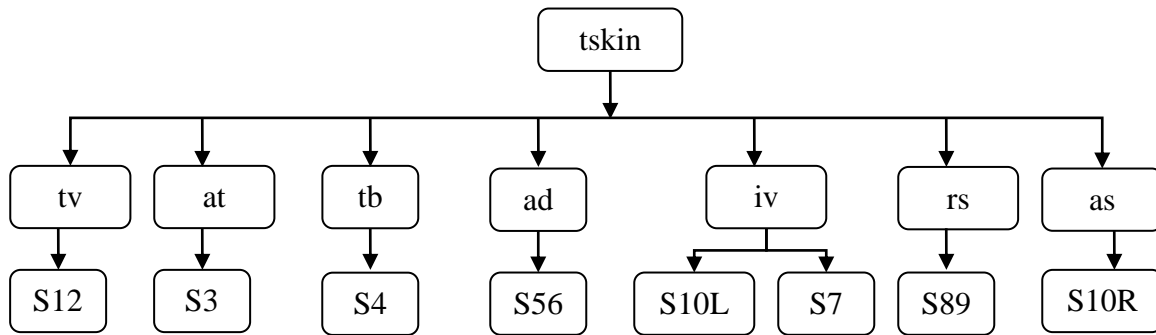


Figure 2: The optimum hierarchy. Note that $S12 = \text{Station1} + \text{Station2}$, $\text{Station56} = \text{Station5} + \text{Station6}$, and $S89 = \text{Station8} + \text{Station9}$, which are composite lymph node zones formed as the union of basic lymph node stations. Also, $tv = tb + vs$, $at = as + tb$, $ad = as + scord$, and $iv = ims + vs$, which are formed as the union of thoracic organ objects.

2.3 Model building

From the definition of each object, the fuzzy anatomy model (*FAM*) of the collection of organs and nodal zones is built as $FAM(B) = (H, M, \rho, \lambda, \eta)$ in the thoracic body region B following [5]. The elements of *FAM* are as follows: H means the hierarchy which is represented as a tree as shown in Figure 1. M is a set of fuzzy models, one fuzzy model for each object in B . ρ represents the relationship of each parent and its child in H . λ is a collection of scale factor ranges, which indicates the size variation of each object in B . The element η represents a set of measurements pertaining to the object assembly in B . See [5] for details.

2.4 Lymph node station recognition

During recognition, we employ two different methods to recognize the organs and lymph node stations: a one-shot method and a thresholded optimal search method [5] [6]. The one-shot method is used to localize the lymph node stations, which makes use of knowledge embedded in $FAM(B)$, including the geometric relationship from parent to child. Firstly, the parent is recognized according to the hierarchy. Subsequently, the location of the child's fuzzy model is found based directly on the parent-child geometric relationship.

In the thresholded optimal search method for organs, the one-shot method is first employed and the refined result is obtained by matching the model to the image by using the optimal range of threshold for each object. In this work, we use thresholded optimal search algorithm to recognize objects (organs and combined organs), which refines the object pose by an optimal search based on the range of threshold which we have introduced in Section 2.3.

3. EXPERIMENTAL RESULTS

Image data

This retrospective study was conducted following approval from the Institutional Review Board at the Hospital of the University of Pennsylvania along with a Health Insurance Portability and Accountability Act waiver. All contrast-enhanced thoracic CT image data sets were selected from our health system patient image database by a board certified radiologist (D.A.T). In this study, we selected 28 contrast-enhanced CT image data sets from our data sets to build the model, and another 12 contrast-enhanced CT image data sets for testing the AAR recognition performance of the 8

lymph node stations. The 40 nearly normal subjects were male patients with an average age of 54.7 ± 3.9 years. Each CT image data set consisted of an average of 58 axial slices covering the entire thorax, with a pixel size of $0.776 \text{ mm} \times 0.776 \text{ mm}$ and a slice spacing of 5 mm. Each of the above organs and lymph node stations was delineated manually according to the corresponding definitions to serve as the ground truth for comparison.

Recognition result

We employ the hierarchy shown in Figure 2 to build the model and recognize the objects and lymph node stations. Figure 3 displays an example of the ground truth (left) and the recognition result (right) for Station3 on the same CT slice through the thorax, and Figure 4 displays an example of the ground truth (left) and the recognition result (right) for Station4 on the same CT slice through the thorax.

Here, two metrics were used to evaluate recognition performance: position error and scale error as defined in [5]. The position error describes the distance between the geometric centers of the ground truth delineation of the lymph node station and the recognition result of the corresponding lymph node station. The scale error is the ratio of the size of the recognition result divided by the size of the true object. Note that the ideal values for these two metrics are 0 and 1, respectively. Mean and standard deviation over the tested data sets are shown in Table 1.

In Table 1, it can be seen that the IASLC-defined thoracic lymph node stations can be localized within about 2 voxels of the ground truth. The scale error is mostly nearly 1 (ideal). The last column represents the mean of the position error and scale error over all thoracic lymph node stations. Note that the second and fourth rows show the standard deviation of error. Compared to the results reported in [3], the recognition result has improved considerably by use of an optimal parent strategy for each lymph node station. Note that the recognition performance was further improved by combining some lymph node stations as shown.

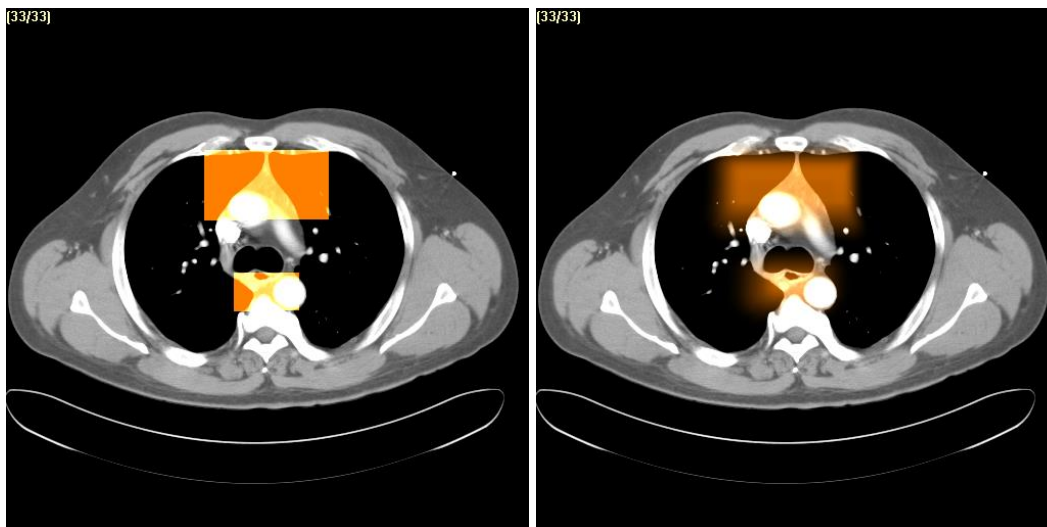


Figure 3: Sample displays of ground truth (left) and Station3 superimposed on thoracic CT image through upper thorax

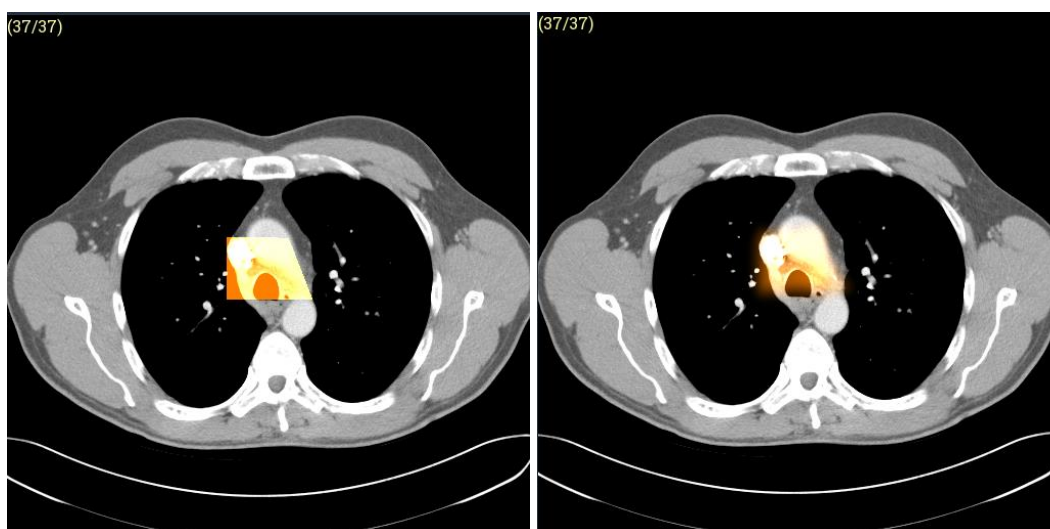


Figure 4: Sample displays of ground truth (left) and Sation4 superimposed on thoracic CT image through upper thorax

Table 1. Position error and scale error (mean and SD) in recognizing IASLC-defined thoracic lymph node stations and thoracic objects on CT images.

| | tskin | tv | at | tb | ad | iv | rs | as | S12 | S3 | S4 | S56 | S7 | S89 | S10R | S10L | Mean |
|----------------------------|-------|------|------|------|-------|------|------|------|-------|------|------|-------|-------|-------|------|-------|------|
| Position Error (mm) | 5.39 | 7.6 | 5.66 | 6.99 | 14.01 | 7.98 | 7.51 | 5.72 | 12.59 | 7.98 | 9.38 | 12.31 | 10.36 | 11.46 | 8.23 | 11.57 | 9.05 |
| | 3.03 | 4.35 | 2.46 | 4.69 | 3.46 | 5.43 | 3.27 | 3.11 | 5.31 | 3.61 | 4.59 | 6.96 | 6.86 | 6.14 | 2.94 | 7.11 | 4.58 |
| Scale Error | 1 | 0.91 | 1.02 | 0.9 | 1.17 | 1 | 0.99 | 1.01 | 0.79 | 0.98 | 0.79 | 1.05 | 1.07 | 1 | 1.01 | 1.03 | 0.98 |
| | 0.01 | 0.06 | 0.1 | 0.09 | 0.08 | 0.04 | 0.02 | 0.08 | 0.18 | 0.08 | 0.06 | 0.09 | 0.1 | 0.07 | 0.08 | 0.05 | 0.07 |

4. CONCLUSIONS

In comparison to our previous work [3], the recognition result for IASLC-defined thoracic lymph node stations has significantly improved, especially for Station12 and Station56. The main new strategies utilized were to combine organs and to find the optimal parent for each lymph node station, which are useful for our AAR framework to recognize the thoracic lymph node stations. We test all possible pair-wise combinations of the organs and find the optimum parent for each lymph node station. It is possible to combine three objects as one parent of the lymph node station and to find the optimal parent in this manner. Our results indicate that a position error of within about 2 voxels is feasible for most of the thoracic lymph node stations on these CT data sets with large slice spacing (5 mm). We believe that it is quite remarkable that the nodal zones can be recognized this accurately considering the variability in their definition and lack of intensity-based border evidence in the image for them. From our early results on disease quantification on PET/CT data sets, recognition error within about two voxels permits accurate delineation-less disease quantification of lymph nodes collectively within a zone, which is our current goal.

5. ACKNOWLEDGEMENTS

This work is supported by an NIH grant R41CA199735-01A1. The training of Mr. Guoping Xu in the Medical Image Processing Group, Department of Radiology, University of Pennsylvania, Philadelphia, for the duration of one year was supported by the China Scholarship Council.

6. REFERENCES

- [1] Nogues I, Lu L, Wang X, et al. Automatic lymph node cluster segmentation using holistically-nested neural networks and structured optimization in CT images[C]//International Conference on Medical Image Computing and Computer-Assisted Intervention. Springer International Publishing, 2016: 388-397.
- [2] Rusch VW, Asamura H., Watanabe H, et al. The IASLC lung cancer staging project: a proposal for a new international lymph node map in the forthcoming seventh edition of the TNM classification for lung cancer. *J Thorac Oncol* 2009;4(5): 568-577.
- [3] Matsumoto M M S, Beiga N G, Udupaa J K, et al. Automatic localization of IASLC-defined mediastinal lymph node stations on CT images using fuzzy models[J]. *system*, 2014, 2: 4.
- [4] Song Y, Udupa J K, Odhner D, et al. Lymph Node Detection in IASLC-defined zones on PET/CT Images[C]//Proc. of SPIE Vol. 2016, 9785: 978515-1.
- [5] Udupa J K, Odhner D, Zhao L, et al. Body-wide hierarchical fuzzy modeling, recognition, and delineation of anatomy in medical images[J]. *Medical image analysis*, 2014, 18(5): 752-771.
- [6] Wang H, Udupa J K, Odhner D, et al. Automatic anatomy recognition in whole - body PET/CT images[J]. *Medical physics*, 2016, 43(1): 613-629.